Spatial dependence of CBV-fMRI: a comparison between VASO and contrast agent based methods

Tao Jin and Seong-Gi Kim
Magnetic Resonance Research Center, Department of Radiology
University of Pittsburgh, Pittsburgh, PA 15203

Abstract

In functional magnetic resonance imaging (fMRI), the cerebral blood volume (CBV) based approach with exogenous contrast agent has been found to have better spatial specificity than the widely applied blood oxygenation level-dependent (BOLD) method. Recently, an endogenous CBV-based contrast, vascular space occupancy-dependent (VASO) technique, was developed for human research. However, the spatial specificity of VASO functional maps is still unclear. In this report, VASO-weighted high-resolution functional map was obtained at 9.4 T. Its spatial dependence across cortical layers was compared to the traditional CBV-weighted fMRI map obtained using contrast agent injection. Both functional maps show good localization at the middle cortical layer.

Keywords: fMRI, VASO, CBV-weighted, MION, cortical-layer-dependence

Introduction

Functional magnetic resonance imaging (fMRI) has experienced rapid growth since its discovery and has become one of the most effective experimental tools for mapping brain activity. To date, the blood oxygenation level-dependent (BOLD) method is by far the most widely used technique in fMRI studies, in which functional changes of the blood deoxyhemoglobin content affect the MR signal by changing the local magnetic field. The signal source of BOLD contrast comes from a combined effect of several physiological changes, such as the cerebral blood flow (CBF), cerebral blood volume (CBV) and oxygen metabolism.

It is generally known that gradient-echo (GE) BOLD, currently the primary methodology for fMRI studies, is inadequate for high–resolution functional mapping of sub-millimeter resolution because there is large signal contribution within and around draining venous vessels. The CBF-fMRI has been shown to have high spatial specificity and to regulate at submillimeter columnar level (1). However, its application in high-resolution fMRI studies is limited by its low signal to noise ratio (SNR) and slow temporal resolution. Using exogenous contrast agent (e.g., monocrystalline iron oxide nanoparticle (MION)) with high susceptibility and long intravascular half-lifetime, CBV-based methods have been widely applied in animal fMRI research. CBV-weighted fMRI with contrast agent injection has been shown to have a much higher sensitivity than BOLD (2,3), and is specific to the middle cortical layer where the microvessel density is the highest (4,5). The CBV-weighted fMRI has also been successfully applied to mapping functional activities at a columnar level (6). However, the application of contrast agent based CBV-fMRI to human research is limited. Recently, another CBV-based technique, vascular space occupancy-dependent (VASO) technique was proposed which is noninvasive and has the potential to be applied in human fMRI. The VASO technique utilizes the difference in the longitudinal relaxation times (T_1) of blood and tissue water. The MR signal of blood water is nulled in an inversion recovery sequence; therefore the change in the blood volume can be detected through the complementary signal change from the remaining tissue. The contrast-to-noise ratio (CNR) of the VASO-fMRI was found to be comparable to CBF-based fMRI at a clinical 1.5 T scanner, and is about 3 times lower than BOLD-fMRI (7). Alternatively, VASO-weighted fMRI without suppressing the blood signal can be applied to enhance the CNR for functional mapping, in which the difference between the longitudinal magnetization (M_z) of blood and tissue can be optimized (8).

Current VASO studies are mostly performed at clinical magnetic fields of 1.5 and 3 T. The detection of VASO contrast at higher field may be difficult because the relative difference between the T_1 of blood and tissue water decreases at higher fields, reducing the VASO contrast (9). In addition, the longer T_1 values of blood and tissue water at higher magnetic fields reduce the steady state signal if the TR is not long enough for a full recovery of the inverted magnetization. For example, the T_1 of blood and tissue water at 9.4 T is 2.2 and 1.9 s (9), respectively. Assuming a repetition time TR = 3 s, the blood and tissue nulling point for a typical VASO sequence would be 1.02 s and 0.96s, respectively. By comparison, the T_1 of blood and tissue water at 1.5 T is 1350 and 1000 ms (7), and the blood and tissue nulling point at TR = 3 s is 797 ms and 645 ms, respectively. At 9.4 T, the SNR will be very low if the exact blood nulling point is used since it is so close to the tissue nulling point. Another factor hampers the detection of VASO signal at high field is that the BOLD signal change is enhanced, which is of opposite sign of the VASO signal change.

Previous VASO-fMRI studies were mostly performed on humans with relatively low spatial resolution using clinical scanners. Although some results have suggested that the functional VASO signal changes are located at the gray matter region (7), it would be valuable to verify its spatial specificity at a higher spatial resolution, and compare with contrast-agent based CBV-fMRI which has been shown to have both columnar and laminar specificities. In this report, we studied VASO-weighted fMRI and MION-fMRI using a cat visual stimulation model at 9.4 T. The aims are: (i) to find whether a functional VASO contrast is detectable at 9.4 T, and (ii) to examine the spatial specificity of the VASO-weighted functional map by comparison with those obtained from MION-fMRI.

Methods

Animal preparation and stimulation

Eleven female adolescent cats were studied under an animal protocol approved by the Institutional Animal Care and Use Committee at the University of Pittsburgh. Details of the animal preparation procedure have been described previously (10). Briefly, the animals were artificially

ventilated under isoflurane (0.8–1.2%). The animal was kept at normal physiological level, and the head was fixed with a homemade head frame with bite and ear bars. For MION-fMRI experiments, 10mg Fe/kg MION was injected intravenously for the CBV-weighting. Visual stimulation was presented binocularly with high contrast drifting square-wave gratings during the stimulation condition. The temporal and spatial frequencies of the gratings are 2 cycles/s and 0.15 cycle/degree. Stationary gratings of the same spatial frequency were presented during the control period.

MR experiments

All MR experiments were performed on a 9.4 T/31-cm horizontal magnet (Magnex, UK) interfaced to a Unity INOVA console (Varian, Palo Alto, CA). For MION experiments, a 1.6-cm diameter surface coil was placed on top of the animal's head for radiofrequency excitation and reception. In VASO-weighted experiments, a Helmholtz head coil was used for inversion and a 1.6-cm surface coil for both excitation and detection, and the two coils were actively detuned.

Fast low-angle shot images were obtained to identify anatomical structures in the brain and to place the region of interest (ROI) close to the isocenter of the magnetic field. Magnetic field homogeneity was optimized by localized shimming. A single 2-mm coronal plane perpendicular to the surface of the cortex that gave a high-quality EPI image as well as robust BOLD contrast was chosen from multi-slice "scout" GE-EPI BOLD fMRI studies. All the subsequent experiments were conducted on that slice with 2×2 cm^2 field of view and 2-mm thickness. For anatomical reference, a T_1 weighted image was acquired by 4-shot spin-echo EPI with a 128×128 matrix.

For MION-fMRI experiments (n = 6 animals), a two-shot GE-EPI sequence was used with a TR of 0.5 s/shot. The scanning matrix was 96×96, which was zero-filled to 128×128 for image reconstruction. Two echo times (TE) of 6 and 10 ms were arrayed in each run, thus the temporal resolution is 2 s. For VASO-fMRI experiments (n = 5 animals), single-shot GE-EPI with inversion pulse preparation was used. The inversion time (TI) = 1.5 s; TR = 3 s; TE = 19 ms; and the scanning matrix = 64×64. A non-selective inversion and a slice-selective inversion was arrayed in each run, thus the temporal resolution is 6 s. The images with non-selective inversion were analyzed for the VASO-weighting results.

VASO-weighted fMRI and MION-fMRI were performed separately due to time restriction. For both studies, the block design stimulation paradigm was 60 s (30 or 10 images) control, 60 s stimulation, and 160 s control. There is ~1 minute resting time between each run. To improve the SNR, ~50 and 20 runs were averaged for VASO-weighted and MION-fMRI experiments, respectively.

Data analysis

Data was analyzed with Matlab® programs and STIMULATE software (11). Student's *t*-test was performed on a pixel-by-pixel basis to detect the activated area. A *t* threshold of 2.0 and a minimal cluster size of three pixels were applied. Signal percent changes were then calculated for the statistically active pixels. For quantitative calculations of the VASO-weighted data, the baseline periods were defined as eight images (48 s) of pre-stimulation data (excluding the 1st and 10th images), while the activation periods were defined as data from 2nd to 10th image (6 s to 60 s) after the onset of stimulation. For MION-fMRI, the baseline periods were 28 images (56 s) of pre-stimulation data (excluding the 1st and 30th images), while the activation periods were defined as data from 5th to 30th image (10 s to 60 s) after the onset of stimulation.

The spatial characteristics of the VASO-weighted fMRI and MION-fMRI maps were analyzed as a function of cortical depth (12). Rectangular sections within area 18 of the visual cortex were first selected (13), pixels were then spatially interpolated along the direction normal to the cortical surface using the nearest-neighbor resampling method (14), and finally the averaged signal profiles across cortical layers were plotted as a function of distance from the surface of the cortex. The data are reported as mean ± standard deviation (SD).

Results and Discussions

Fig. 1A showed the signal percent change map of one representative animal obtained from the MION-fMRI experiment. Activated pixels with negative signal change were observed at the primary visual cortex, where the gray matter area was depicted by the green contour. The signal decrease is due to a functional increase of the CBV and consequently the field inhomogeneity induced by the high susceptibility of blood. The activation dominates at the middle of the cortex, in agreement with previous CBV-weighted studies (5).

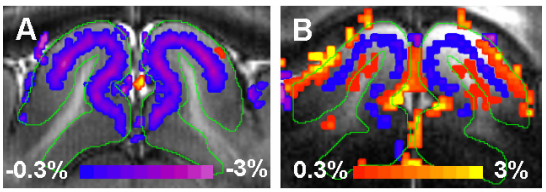

Fig. 1 Signal percent change maps obtained from the MION-fMRI (TE = 6 ms) (A) and VASO-weighted fMRI (B), overlaid on T_1-weighted images.

Fig. 1B shows the VASO-weighted signal change map overlaid on a T_1-weighted image. In contrast to the MION-fMRI, both positively and negatively activated pixels were detected. The signal increase at the cortical surface as well as at the boundary of the gray-white matter is due to the BOLD contribution since our TE is relatively long. A nice band of signal-decreasing pixels located exactly at the middle of the cortex indicating that the contribution from the VASO-weighting signal dominates in this region, although the signal change is relatively small. This is drastically different from those typical GE-BOLD functional maps, and confirms that VASO-weighted contrast can be detected at a high magnetic field of 9.4 T. In our VASO-weighting sequence, there are

mainly two contributions to the fMRI signal changes: the inversion preparation (with 1.5 s TI) gives the VASO-weighting, and the GE-EPI acquisition gives BOLD contribution. The GE-BOLD contribution is much more significant at the surface than at the middle cortical layer (5), while the VASO-induced signal decrease is more significant at the middle cortical layer, similar to the MION-fMRI results in Fig. 1A.

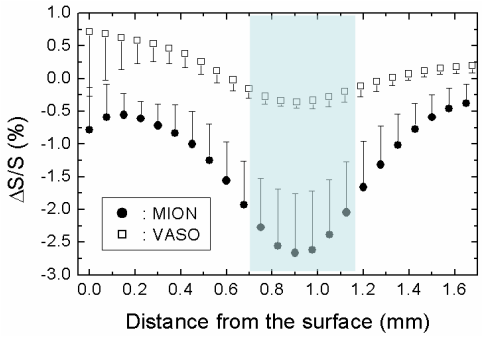

Fig. 2 The cortical-depth dependence of the signal percent changes measured by the VASO-weighted fMRI and MION-fMRI. The blue shaded region indicates the layer IV of the visual cortex. Only half of the error bar was shown.

The signal percent changes as a function of cortical depth are shown in Fig. 2. The MION-fMRI shows large signal decrease at the middle cortical layer, centered at ~0.9 mm from the cortical surface, nearly the middle of the layer IV of the cat visual cortex which ranges from 0.7 to 1.15 mm (15). The full width at half maximum (FWHM) of the averaged peak was measured to be 0.65 mm. Although there is significant positive BOLD signal at the cortical surface, the VASO-weighted signal change also exhibited a negative peak at the middle of layer IV, suggesting that BOLD contribution to the VASO-weighted signal does not significantly distort the profile of CBV responses across the cortex. While the peak intensity is much smaller (<0.5%), the peak position (~0.9 mm) and the FWHM (~0.7 mm) are very similar to the MION-fMRI results, suggesting that both methods detected similar functional CBV change. The VASO-induced signal decrease at the middle cortical layer can be enhanced by using a shorter TE to reduce the BOLD effects.

Although a VASO-type of functional contrast was detected in our experiments, its signal source needs further examination. In a typical VASO experiment which uses a full body inversion pulse, the inflow effect of the blood water is minimal, and the steady state magnetization as a function of TR and TI is

$$M_{z,full}=M_0\cdot[1-2\cdot\exp(-TI/T_1)+\exp(-TR/T_1)] \quad [1]$$

for both blood and tissue water (7). Here the subscript "full" indicates a full body inversion. Since a head coil was used in our VASO-weighted experiments, the non-selective inversion pulses only invert spins within the coverage of the coil. Hence the effect of the inflow of non-inverted blood water spins from outside the coil should be considered. It has been shown in a human study that the effect of this inflow on VASO-fMRI is minimal when a relatively thick inversion slab is used (16). In our cases, the inflow effect will depend on the TR, TI, and the transit time ($t_{transit}$) of non-inverted spins to the imaging slice. The transit time is related to the blood velocity, vascular characteristics and the coil coverage, and is difficult to be measured accurately. However, the signal behavior can be qualitatively divided into three regimes as follows: (1) $t_{transit} < TI$, fresh spins move to the imaging slice and replace all the inverted spins before the excitation pulse is applied, the magnetization of blood water being excited and imaged is equal to the fully non-inverted magnetization, $M_{z,1} = M_0$. In this scenario, which is usually the case when the inversion slab is very thin and/or a very long TI is used, there will be no VASO contrast because the blood signal cannot be nulled, and a functional increase of the MR signal would be expected due to the increase of CBF. (2) $TI < t_{transit} < TR$, fresh spins move to the imaging slice and replace all the inverted blood water spins after the excitation and imaging, and therefore the inversion pulse inverted fresh spins (M_0) each time. The magnetization of blood water becomes: $M_{z,2}=M_0\cdot[1-2\cdot\exp(-TI/T_1)]$. The blood-nulling point in this case becomes $T_1\cdot\ln 2$, which is ~1.5s at 9.4 T and equals to the value used in our VASO-fMRI experiments, significantly larger than the null point of 1.02 s from a full body inversion. For (3) $t_{transit} > TR$, the situation would become more complicated. The magnetization of the blood water in the imaging slice before the excitation will be between $M_{z,2}$ and $M_{z,s}$, and may also be spatially dependent. In all the above scenarios, the magnetization of the tissue water within the imaging slice would be the same as in Equation [1] if the effect of the exchange between the tissue and blood water is negligible.

For a typical VASO experiment with full body inversion, the detection of a functional VASO contrast would be difficult at 9.4 T due to the small difference in the T_1 of blood and tissue water and the enhanced BOLD effect at high field. Assuming normal physiological changes during activation, a simulation predicts a slightly positive signal change at the middle layer of the visual cortex using our experimental parameters (results not shown). The significant signal decrease at the middle cortical layer we observed may be explained by either scenario (2) or (3), where VASO-weighting effect would be enhanced because the T_1 difference between the blood and tissue water can be considered as effectively enlarged. Further studies are needed to better understand the observed VASO-weighted signal, and may help to improve the application of the VASO-fMRI.

Conclusions

VASO-weighted fMRI changes were detected at 9.4 T. Despite a low CNR and BOLD contamination, VASO-weighted functional map shows clear negative signal changes at the middle cortical layer, similar to the spatial localization of the maps obtained by the contrast agent method, indicating that the VASO-based technique detects similar CBV changes as the contrast agent based methods, and can potentially be applied to high-resolution functional mapping.

Acknowledgments

The authors thank Dr. Jicheng Wang for building RF coils and acquiring some preliminary data. This work is supported by NIH grants EB003324, EB003375, RR17239, NS44589 and EB002013.

References:

1. Duong TQ, Kim D-S, Ugurbil K, Kim S-G. Localized cerebral blood flow response at submillimeter columnar resolution. Proc Natl Acad Sci USA 2001;98:10904-10909.
2. Mandeville JB, Marota JJA, Kosofsky BE, Keltner JR, Weissleder R, Rosen BR. Dynamic functional imaging of relative cerebral blood volume during rat forepaw stimulation. Magn Reson Med 1998;39:615-624.
3. Vanduffel W, Fize D, Mandeville JB, Nelissen K, van Hecke P, Rosen BR, Tootell RBH, Orban GA. Visual motion processing investigated using contrast agent-enhanced fMRI in awake behaving monkeys. Neuron 2001;32:565-577.
4. Lu HB, Patel S, Luo F, Li SJ, Hillard CJ, Ward BD, Hyde JS. Spatial correlations of laminar BOLD and CBV responses to rat whisker stimulation with neuronal activity localized by Fos expression. Magnetic Resonance in Medicine 2004;52(5):1060-1068.
5. Zhao F, Wang P, Hendrich K, Ugurbil K, Kim S-G. Cortical layer-dependent BOLD and CBV responses measured by spin-echo and gradient-echo fMRI: Insights into hemodynamic regulation. Neuroimag 2006:1149-1160.
6. Zhao F, Wang P, Hendrich K, Kim S-G. Spatial specificity of cerebral blood volume-weighted fMRI responses at columnar resolution. 2005. p 416-424.
7. Lu H, Golay X, Pekar J, Van Zijl P. Functional magnetic resonance imaging based on changes in vascular space occupancy. Magn Reson Med 2003;50:263-274.
8. Wu W-C, Wegener S, Buxton RB, Wong EC. Vascular space occupancy weighted imaging with control of inflow effect and higher signal-to-noise ratio. 2006; ISMRM, Seattle. p 2768.
9. Tsekos NV, Zhang F, Merkle H, Nagayama M, Iadecola C, Kim S-G. Quantitative measurements of cerebral blood flow in rats using the FAIR technique: Correlation with previous iodoantipyrine autoradiographic studies. Magn Reson Med 1998;39:564-573.
10. Jin T, Wang P, Tasker M, Zhao F, Kim S-G. Source of Nonlinearity in Echo-Time-Dependent BOLD fMRI. Mag Reson Med 2006;55:1281-1290.
11. Strupp JP. Stimulate: A GUI based fMRI analysis software package. NeuroImage 1996;3:S607.
12. Zhao F, Wang P, Kim S-G. Cortical depth-dependent gradient-echo and spin-echo BOLD fMRI at 9.4T. Magn Reson Med 2004;51:518-524.
13. Bonhoeffer T, Grinvald A. The layout of iso-orientation domains in area 18 of cat visual cortex: optical imaging reveals a pin-wheel-like organization. J Neurosci 1993;13:4157-4180.
14. Tsao J. Interpolation Artifacts in Multimodality Image Registration Based on Maximization of Mutual Information. IEEE Trans Med Imaging 2003;22:854-864.
15. Payne BR, Peters A. The Concept of Cat Primary Visual Cortex. In: Payne BR, Peters A, editors. The Cat Primary Visual Cortex: Academic Press; 2002. p 1-129.
16. Yang YH, Gu H, Stein EA. Simultaneous MRI acquisition of blood volume, blood flow, and blood oxygenation information during brain activation. Magnetic Resonance in Medicine 2004;52(6):1407-1417.